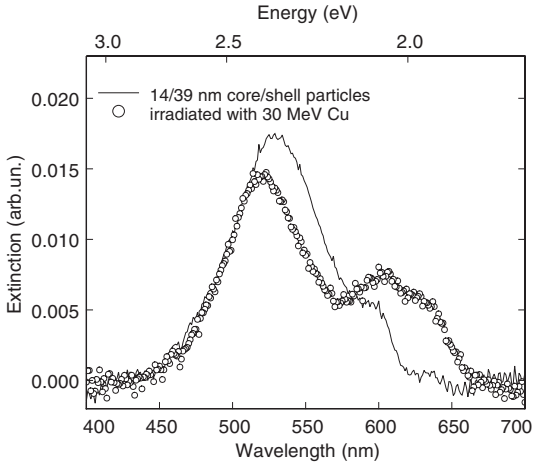

Figure 4. Optical extinction spectra for ensembles of core–shell colloids with 14 nm diameter Au cores and 39 nm thick shells embedded in an index-matching fluid. Data are shown before and after irradiation with 30 MeV Cu ions. A broadening of the plasmon absorption band is observed, which is attributed to the formation of Au nanorods.

In conclusion, mega-electron-volt ion irradiation of colloidal silica particles containing an Au core leads to a deformation of the shell into an oblate ellipsoid and of the Au core into a nanorod. The Au deformation is attributed to the in-plane mechanical stress in the silica shell acting on the radiation-softened Au core. The Au nanorods have size aspect ratios as large as nine for intermediate fluences; they break up for higher fluences. Preliminary optical extinction data show surface plasmon resonance shifts characteristic for anisotropic Au nanorods. As anisotropic deformation is known to occur in a variety of (amorphous) hosts, several other combinations of core and shell materials may be ion-beam-shaped as well.

Experimental

Materials: Colloidal core–shell particles were prepared in solution using a method described elsewhere [12]. A few drops of the solution were allowed to dry on a quartz substrate. Scanning electron microscopy (SEM) and Rutherford backscattering spectrometry were used to confirm that at least ten layers of colloidal particles covered the surface of these substrates. It was also evident that the colloid layer thickness varied across the samples due to inhomogeneous deposition and drying conditions. A few drops of a diluted solution were dispersed on a 10 nm thick Si_3N_4 membrane which allowed transmission electron microscopy (TEM) of individual particles.

Ion Irradiation: The particles were irradiated with 30 MeV Cu or Se ions to fluences in the range $2–4 \times 10^{14}$ ions cm^{-2}. During irradiation the samples were clamped to a liquid-nitrogen-cooled Cu block. Some irradiations were done at normal incidence, others with the ion beam 20° or 45° tilted away from the normal. 6 MV tandem accelerators in Rossendorf and Montreal provided the ion beams. Following irradiation the colloids were examined by SEM (5 keV electron beam), TEM (200 keV electron beam), and optical transmission measurements.

Received: July 23, 2003
Final version: October 16, 2003

[1] P. Mulvaney, *MRS Bull*. **2001**, *26*, 1009.
[2] C. Sönnichsen, T. Franzl, T. Wilk, G. von Plessen, J. Feldmann, O. Wilson, P. Mulvaney, *Phys. Rev. Lett*. **2002**, *88*, 077 402.
[3] K. P. Yuen, M. F. Law, K. W. Yu, P. Sheng, *Phys. Rev.* **1997**, *E56*, 1322.
[4] B. M. I. van der Zande, L. Pages, R. A. M. Hikmet, A. van Blaaderen, *J. Phys. Chem. B* **1999**, *103*, 5761.
[5] E. Snoeks, A. van Blaaderen, T. van Dillen, C. M. van Kats, M. L. Brongersma, A. Polman, *Adv. Mater*. **2000**, *12*, 1511.
[6] A. Benyagoub, S. Klaumünzer, L. Thomé, J. C. Dran, F. Garrido, A. Dunlop, *Nucl. Instr. Methods* **1992**, *64*, B684.
[7] T. van Dillen, A. van Blaaderen, W. Fukarek, A. Polman, *Appl. Phys. Lett*. **2001**, *78*, 910.
[8] H. Trinkaus, A. I. Ryazanov, *Phys. Rev. Lett.* **1995**, *74*, 5072.
[9] M. L. Brongersma, E. Snoeks, A. Polman, *J. Appl. Phys*. **2000**, *88*, 59.
[10] E. Snoeks, K. S. Boutros, J. Barone, *Appl. Phys. Lett*. **1997**, *71*, 267.
[11] C. F. Bohren, D. R. Hoffman, *Absorption and Scattering of Light by Small Particles*, Wiley, New York **1983**, Ch. 12.
[12] a) L. M. Liz-Marzan, M. Giersig, P. Mulvaney, *Langmuir* **1996**, *12*, 4329. b) C. Graf, D. L. Vossen, A. Imhof, A. van Blaaderen, *Langmuir* **2003**, *19*, 6693.

Porous Tin Oxides Prepared Using an Anodic Oxidation Process**

By *Heon-Cheol Shin*, *Jian Dong*, and *Meilin Liu**

The formation of self-ordered porous oxide by an anodization process has been studied for several decades. To date, however, only a few metals, for instance Al[1] and Ti,[2] have been successfully oxidized to form highly ordered porous oxide structures such as honeycomb or nanotubular structures. Porous anodic alumite has been widely used as a template for preparation of many functional materials in nanostructured forms for optical, electronic, magnetic, and electrochemical applications,[3–5] whereas porous anodic titanate could be used for catalytic and gas-sensing applications.[6]

Tin oxide is a semiconductor that has been widely used for various applications, including solid-state gas sensors, optical devices, and lithium secondary batteries.[6–8] A variety of preparation methods have been explored to fabricate nanostructured tin oxides to dramatically improve the desired functionality. In particular, one-dimensional (1D) tin oxide structures such as nanoribbons, nanotubes, and nanorods have been successfully synthesized by a high-temperature thermal oxidation process[9,10] and low-temperature solution-based synthesis[11] for highly sensitive gas sensors in many applications. However, 1D porous tin oxides have not yet been synthesized. In

[*] Prof. M. Liu, Dr. H.-C. Shin, Dr. J. Dong
Center for Innovative Fuel Cell and Battery Technologies
School of Materials Science and Engineering
Georgia Institute of Technology
Atlanta, GA 30332-0245 (USA)
E-mail: meilin.liu@mse.gatech.edu

[**] This work was supported by Office of Science, Department of Energy under Grant No. DE-FG02-01ER15220.

DOI: 10.1002/adma.200305660

ADVANCED MATERIALS

this communication, we report for the first time the creation of meso- to macroporous tin oxides by anodic oxidation of pure tin metal in the trans-passive region.

Shown in Figure 1 are the surface views of tin oxide films prepared by an anodization process, imaged using a scanning electron microscope (SEM; Hitachi S-800 FEG SEM). The nano-sized pores, ranging from 30 to 60 nm, are randomly distributed across the surface. It is noted that the anodic tin oxide has nanochannels almost perpendicular to the substrate, as seen in Figure 2b. However, the channels are discontinuous, since the porous tin oxide is composed of stacked layers of several hundreds nanometers. It is also apparent from the cross-sectional view that numerous small gaps or disk-shaped pores are present between the layers.

The discontinuous nanochannel structure is due probably to the disturbance of the formation of tin oxides by vigorous oxygen evolution under severe anodizing conditions. The rapid liberation of oxygen could create turbulence in the electrolyte and/or local stresses around the oxide/metal interface as porous tin oxide is formed, destroying the long-range order of the nanochanneled structure. These additional pores between the layers could facilitate gas and liquid transport through the porous film for electrochemical or catalytic applications.

In order to explore the detailed structures of the anodized samples, the top and side views of the porous tin oxide films were examined using a transmission electron microscope (TEM; Hitachi HF-2000 TEM). It is noted that the shape of the pores is irregular, as seen in Figure 3a, and the channels are not straight, with varying channel wall thickness, as seen in Figure 3b.

Unlike porous alumite, which is characterized by a centrally situated *circular* pore in an ordered *hexagonal* unit cell, the pore shapes of the anodic tin oxide are irregular, varying from triangular to hexagonal. Assuming that the honeycomb channel structure has 30–60 nm (in diameter) *hexagonal* pores and 5–10 nm thick channel walls, the porosity of the anodic tin oxide is estimated to be 52–83 %, which is much larger than that of porous alumite (about 24 %).[12] In fact, the actual porosity could be even higher when the gaps between the tin oxide layers are taken into consideration. The anodic tin oxide films typically have a surface area of 99.1 $m^2 g^{-1}$, as determined by the Brunauer–Emmett–Teller (BET)[13] technique (ASAP 2000, Micromeretics) using scratched powder of the tin oxide films. The high porosity and large specific surface

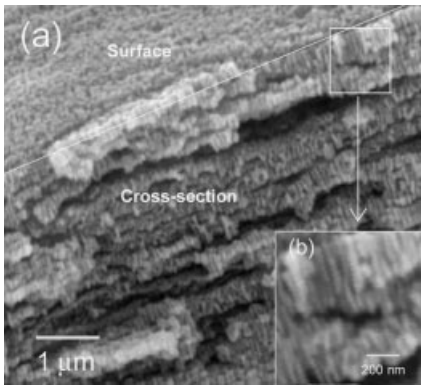

Figure 2. A cross-sectional view of anodic porous tin oxide showing nano-channeled structure and numerous disk-shaped gaps between the layers.

area are ideally suited to electrochemical and catalytic applications. Furthermore, they can be used as a template for preparation of other functional materials in nanostructured forms.

Shown in Figure 4 is a top view of the anodic tin oxide sample annealed at 500 °C for 3 h. The microscopic features of the annealed sample are essentially the same as those of the as-prepared samples: the channel diameter and the wall thickness remained the same (30–60 and 5–10 nm, respectively), implying that the porous structure has good thermal stability. Both the electron diffraction patterns (the insets in Figs. 3a,4) and the X-ray diffraction patterns (Philips PW-1800 X-Ray Diffractometer), as shown in Figure 5, indicate that the as-prepared amorphous tin oxide can be transformed to a crystalline stannic structure (cassiterite SnO_2) by annealing at 500 °C for 3 h.

As shown in Figure 6, the thicknesses of the porous tin oxide layers increase linearly with the applied anodizing voltage and time. Well-defined meso- to macroporous channels were produced with little structural difference when the anodizing voltage was greater than 5 V, which corresponds to the trans-passive region where there is a significant increase in current density as the potential becomes more positive than the passive region. Although similar porous structures were produced at voltages above 12 V, the resulting films had poor adhesion to the substrate and were often delaminated from the substrate during anodizing or the subsequent drying/handling process. The poor adhesion is due probably to more vig-

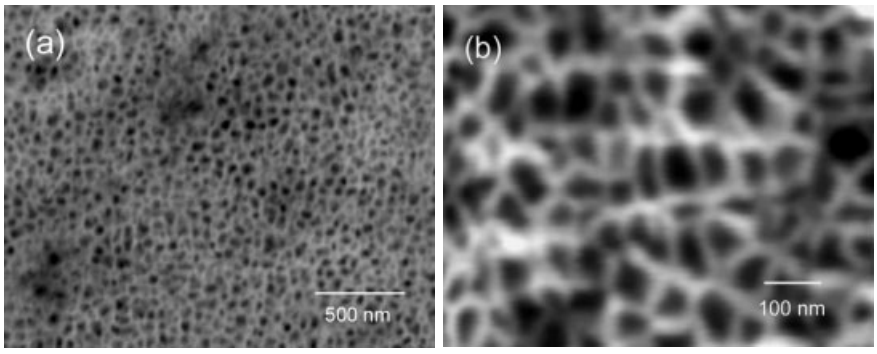

Figure 1. Typical surface views (SEM images) of meso- to macroporous tin oxide created by an anodic oxidation process.

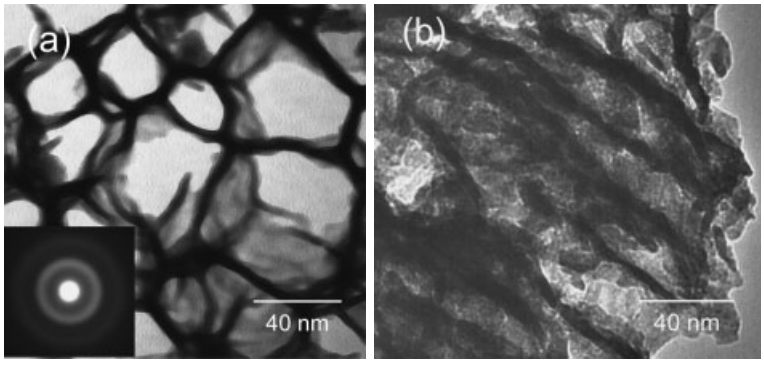

Figure 3. a) Top view and b) side view (TEM images) of the as-prepared porous tin oxides created by anodization. The inset in (a) is an electron diffraction pattern of the wall, indicating the amorphous structure of the as-prepared tin oxides.

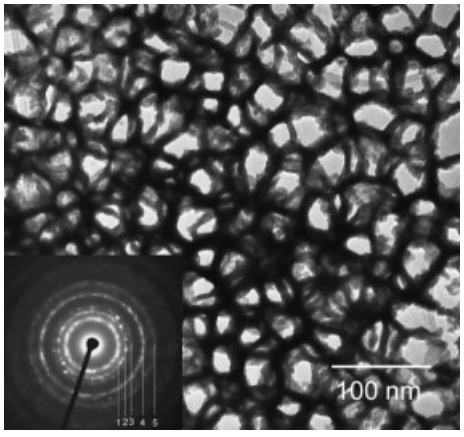

Figure 4. TEM image (top view) of anodic porous tin oxide after annealing at 500 °C for 3 h. The inset is an electron diffraction pattern of the wall and the numbers represent the reflection from different crystallographic planes of cassiterite SnO_2: 1: (200), 2: (211), 3: (002), 4: (222), and 5: (402).

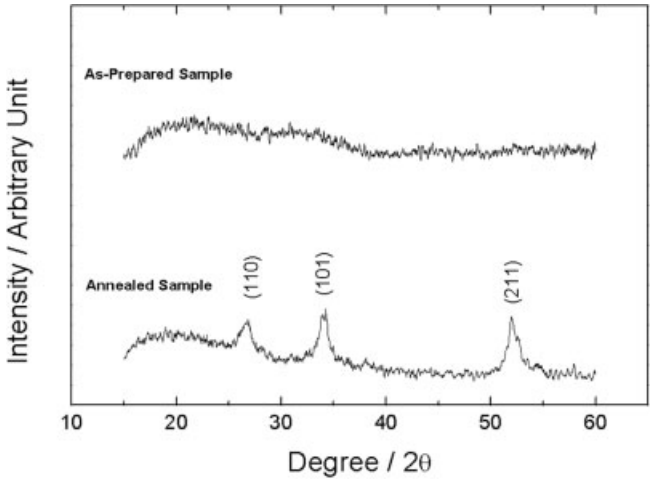

Figure 5. X-Ray diffractograms of as-prepared (upper) and annealed (lower) powders scratched from the substrates. The as-prepared amorphous tin oxide can be transformed to a crystalline stannic structure (cassiterite SnO_2) by annealing at 500 °C for 3 h. Further details of the crystal structure investigation(s) may be obtained from the Fachinformationszentrum Karlsruhe, D-76344 Eggenstein-Leopoldshafen (Germany), on quoting the depository numbers CSD-413242.

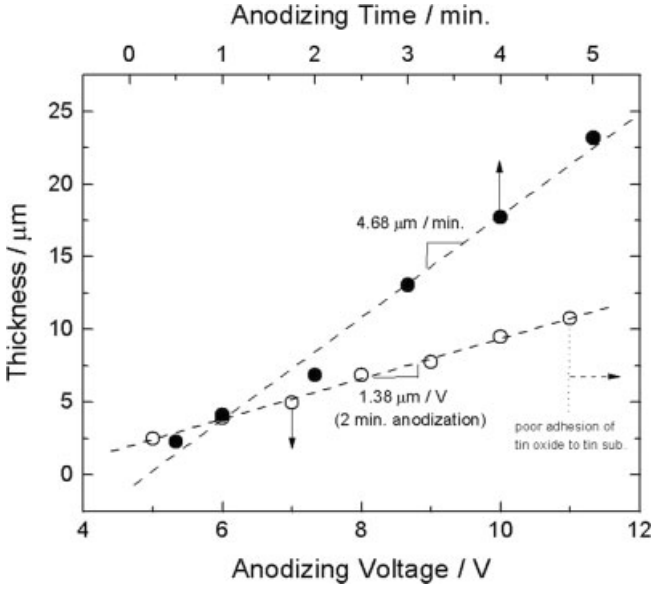

Figure 6. Dependence of thicknesses of the anodic porous tin oxide films on the applied anodizing voltage and time.

orous O_2 evolution near the oxide/tin–substrate interface. From the linear relationship between film thickness and anodizing time, the growth rate of the porous tin oxide film is estimated to be about 78 nm s^{-1}, much faster than the rate reported for the formation of anodic porous alumite (< 5 nm s^{-1}).[14–16]

Although the formation mechanism of the porous tin oxide is yet to be determined, the one-dimensional character of the channels appears to be similar to those found in anodic alumite. The formation of the porous channels is most likely enhanced by the applied electric field for anodization, as observed in alumite.[1,17,18] Considering a typical three-layer configuration (Al | Al oxide | anodizing solution) for the anodization process, both the transport of oxygen-containing anions (O^{2-}/OH^-) from the solution/oxide interface to oxide/Al interface and the migration of Al^{3+} from Al/oxide interface to oxide/solution interface would be enhanced by the applied electric field. The transport of O^{2-}/OH^- contributes to the oxide formation at the interface between Al and Al oxide, while the migration of Al^{3+} to the solution leads to the disso-

ADVANCED MATERIALS

lution of Al. Since the electric field strength across the channel bottom (i.e., the barrier layer) is much greater than that across the channel wall, the Al dissolution rate at the bottom is far greater than that at the wall, resulting in perpendicular growth of the channel with high aspect ratio.

However, other structural features of the anodic tin oxide such as gaps between the oxide layers, irregular pore shape, and a wide range of pore sizes imply that the formation of porous tin oxides is more complicated than that of porous anodic alumite, which is characterized by continuous channels consisting of regular shaped pores with a narrow size distribution. Vigorous gas evolution possibly plays a significant role in creating the irregular porous structure. It is also noted that the growth rate of anodic tin oxide is much faster than that of anodic alumite. Further investigations are needed to characterize the physical and microscopic properties of the barrier layer, the defective nature of tin oxide, and the conductivities of ions (O^{2-}/OH^- and Sn ions) through the tin oxide film, which are critical to clarifying the growth mechanism.

In conclusion, porous tin oxides with nanochannels have been successfully prepared using an anodic oxidation process. This represents a novel way of creating porous structures that allow fast transport of gas/liquid and rapid electrochemical reactions due to high surface area. The present tin oxides with additional pores between the layers are ideally suited for electrodes in electrochemical devices such as batteries and chemical sensors. In particular, the as-prepared and annealed porous tin oxides are being directly used as meso- to macroporous anodes for lithium secondary batteries and the annealed tin oxide with stannic form is being tested for solid-state gas sensors. The electrochemical and catalytic properties of these unique structures will be reported in subsequent communications. Furthermore, the porous tin oxide can be used as a template for preparation of other functional materials in nanostructured forms.

Experimental

High-purity tin (Alfa Aesar, 99.998 %) was used as the working electrode (the anode). Before anodizing, the tin surface was polished to a mirror finish with 1.0 and 0.3 μm alumina powder (in order to remove the native oxide film) and then rinsed in distilled water. A platinum wire was used as the counter electrode (the cathode) for anodization. The distance between anode and cathode was kept at 1 cm. A constant voltage (5 to 14 V) was applied to the substrate using a Solartron 1285 potentiostat in an electrolyte of 0.5 M oxalic acid (Aldrich) at room temperature. Anodization was performed in a stationary electrolyte solution without stirring or N_2 bubbling. After anodization, some samples were annealed at 500 °C for 3 h. Elemental analysis of as-prepared and annealed samples with an energy dispersive X-ray spectrometer (EDS) showed that the only constituents of the samples are tin and oxygen. The as-prepared samples appear to be dark brown, indicating the presence of stannous oxide (SnO) in the sample [19]. In contrast, the annealed samples appear to be white, implying that it is close to stoichiometric stannic oxide (SnO_2).

Received: July 7, 2003
Final version: October 12, 2003

[1] J. P. O'Sullivan, G. C. Wood, *Proc. R. Soc. London, Ser. A* **1970**, *317*, 511.
[2] D. Gong, C. A. Grimes, O. K. Varghese, W. Hu, R. S. Singh, Z. Chen, E. C. Dickey, *J. Mater. Res.* **2001**, *16*, 3331.
[3] T. M. Whitney, J. S. Jiang, P. C. Searson, C. L. Chien, *Science* **1993**, *261*, 1316.
[4] P. Hoyer, N. Baba, H. Masuda, *Appl. Phys. Lett.* **1995**, *66*, 2700.
[5] H. Masuda, H. Asoh, M. Watanabe, K. Nishio, M. Nakao, T. Tamamura, *Adv. Mater.* **2001**, *13*, 189.
[6] A. M. Azad, S. A. Akbar, S. G. Mhaisalkar, L. D. Birkefeld, K. S. Goto, *J. Electrochem. Soc.* **1992**, *139*, 3690.
[7] P. Olivi, E. C. Pereira, E. Longo, J. A. Varella, L. O. de S. Bulhoes, *J. Electrochem. Soc.* **1993**, *140*, L81.
[8] Y. Idota, T. Kubota, A. Matsufuji, Y. Maekawa, T. Miyasaka, *Science* **1997**, *276*, 1395.
[9] M. Law, H. Kind, B. Messer, F. Kim, P. D. Yang, *Angew. Chem. Int. Ed.* **2002**, *41*, 2405.
[10] Z. R. Dai, J. L. Gole, J. D. Stout, Z. L. Wang, *J. Phys. Chem. B* **2002**, *106*, 1274.
[11] F.-F. Zhang, L.-D. Sun, J.-L. Yin, C.-H. Yan, *Adv. Mater.* **2002**, *15*, 1022.
[12] Irrespective of the electrolyte chosen, the pore spacing and pore diameter of anodic alumite are proportional to the anodizing voltage with proportionality constants of 2.5 nm V^{-1} and 1.29 nm V^{-1}, respectively. a) K. Ebihara, H. Takahashi, M. Nagatama, *J. Met. Finish. Soc. Jpn.* **1983**, *34*, 548. b) D. Crouse, Y.-H. Lo, A. E. Miller, M. Crouse, *Appl. Phys. Lett.* **2000**, *76*, 49. Accordingly, porosity of the anodic alumite is relatively insensitive to the anodizing voltage and electrolyte chosen.
[13] SEM images of the scratched powder showed that the anodic tin oxides were in the form of disk-shaped agglomerates with a thickness of several hundreds of nanometers and a length of several tens to hundreds of micrometers. This indicates that the increase in surface area due to scratching of the oxides is relatively small.
[14] H. Masuda, F. Hesegwa, S. Ono, *J. Electrochem. Soc.* **1997**, *144*, L127.
[15] O. Jessensky, F. Muller, U. Gösele, *Appl. Phys. Lett.* **1998**, *72*, 1173.
[16] M. T. Wu, I. C. Lue, M. H. Hon, *J. Vac. Sci. Technol. B* **2002**, *20*, 776.
[17] J. Siejka, C. Ortega, *J. Electrochem. Soc.* **1997**, *124*, 883.
[18] V. P. Parkhutik, V. I. Shershulsky, *J. Phys. D: Appl. Phys.* **1992**, *25*, 1258.
[19] L. Young, *Anodic Oxide Films*, Academic Press, London, New York **1961**, p. 326.

Thermally Assisted Sub-10 fs Electron Transfer in Dye-Sensitized Nanocrystalline TiO_2 Solar Cells**

By *William Stier*, *Walter R. Duncan*, and *Oleg V. Prezhdo**

Elucidating the properties of the interface between traditional inorganic solid-state conductors and novel organic

[*] Prof. O. V. Prezhdo, Dr. W. Stier, W. R. Duncan
Department of Chemistry, University of Washington
Seattle, WA 98195-1700 (USA)
E-mail: prezhdo@chem.washington.edu

[**] The research was supported by NSF, CAREER Award CHE-0094012. OVP is a Camille and Henry Dreyfus New Faculty and an Alfred P. Sloan Fellow.

  DOI: 10.1002/adma.200306027